

## TI Designs: TIDA-01057

# 用于最大限度提高 20 位 ADC 的信号动态范围以实现真正 10V<sub>PP</sub> 差分输入的参考设计



### 说明

此高性能数据采集 (DAQ) 参考设计可提高 20 位差分输入模数转换器 (ADC) 的动态范围。许多 DAQ 系统都需要具有较宽的满标量程 (FSR) 测量能力以获得充足的信号动态范围。在早期的参考设计中, 许多逐次逼近型寄存器 (SAR) ADC 曾采用 THS4551 全差分放大器 (FDA); 然而, THS4551 仅限于 5.4V 的最大电源电压, 这不足以实现真正的 10V<sub>PP</sub> 差分输出 (10V FSR), 因此这需要提高具有 5V 基准电压的 SAR ADC 最大动态范围。此参考设计实现了一款具有 12.6V 最大电源电压的 TI THS4561 FDA 器件, 并通过该器件展示了真正 10V<sub>PP</sub> 差分输出的多个优势。测试结果表明, 与之前的设计 (TIDA-01054) 相比, 该设计不仅可以实现更出色的性能, 同时还降低了总体功耗。

### 资源

[TIDA-01057](#)  
[THS4561](#)  
[ADS8900B](#)  
[REF6050](#)

设计文件夹  
产品文件夹  
产品文件夹  
产品文件夹



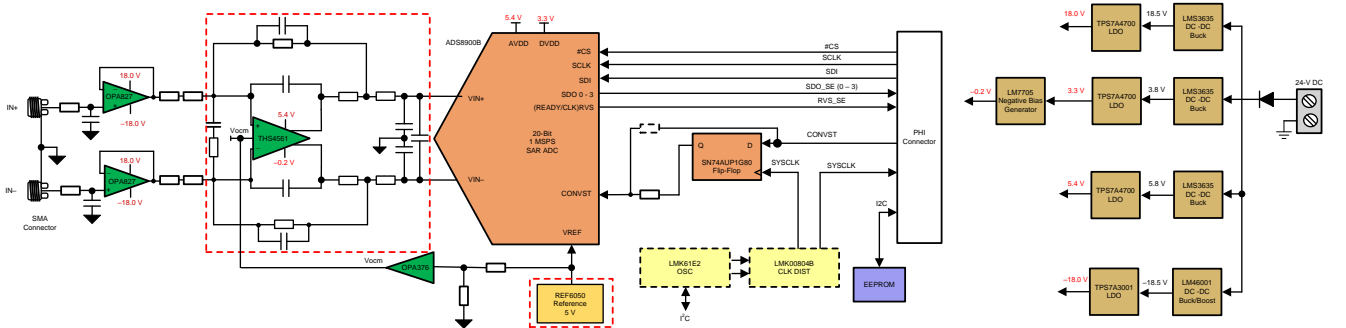
咨询我们的 E2E™ 专家

### 特性

- 20 位 ADC 的真正 10V<sub>PP</sub> 差分模拟前端
- 适用于高通道数系统的模块化前端参考设计 (可重复)

### 应用

- 数据采集 (DAQ)
- 半导体测试设备
- LCD 测试设备
- 实验室仪表
- 电池测试



Copyright © 2018, Texas Instruments Incorporated



该 TI 参考设计末尾的重要声明表述了授权使用、知识产权问题和其他重要的免责声明和信息。

## 1 System Description

Multi-input systems that require the simultaneous or parallel sampling of many data channels present design challenges to engineers developing data acquisition (DAQ) modules and automatic testers for applications such as semiconductor tests, memory tests, liquid-crystal display (LCD) tests, and battery tests. In these systems, often hundreds or thousands of data channels are required; thus, maximizing the signal-to-noise ratio (SNR) performance while minimizing power, component count, and cost are all key design criteria. The analog front-end (AFE) signal chain often consists of a series of muxes, a scaling or programmable gain amplifier (PGA) followed by an anti-aliasing, noise limiting, low-pass filter (LPF), which is paired with the appropriate analog-to-digital (ADC) driver prior to digitization. The ADC converts the time-varying analog input to either a serial or parallel binary bit stream, which is then passed to the embedded host controller (microcontroller (MCU) or field-programmable gate array (FPGA)). Depending on the application, the ADC may contain the necessary reference or the associated buffer integrated as part of the ADC. Furthermore, the designer can also integrate portions of or the entire AFE as a single device for specific applications; however, note that this integration can also limit flexibility.

图 1 shows a block diagram of a generic AFE.

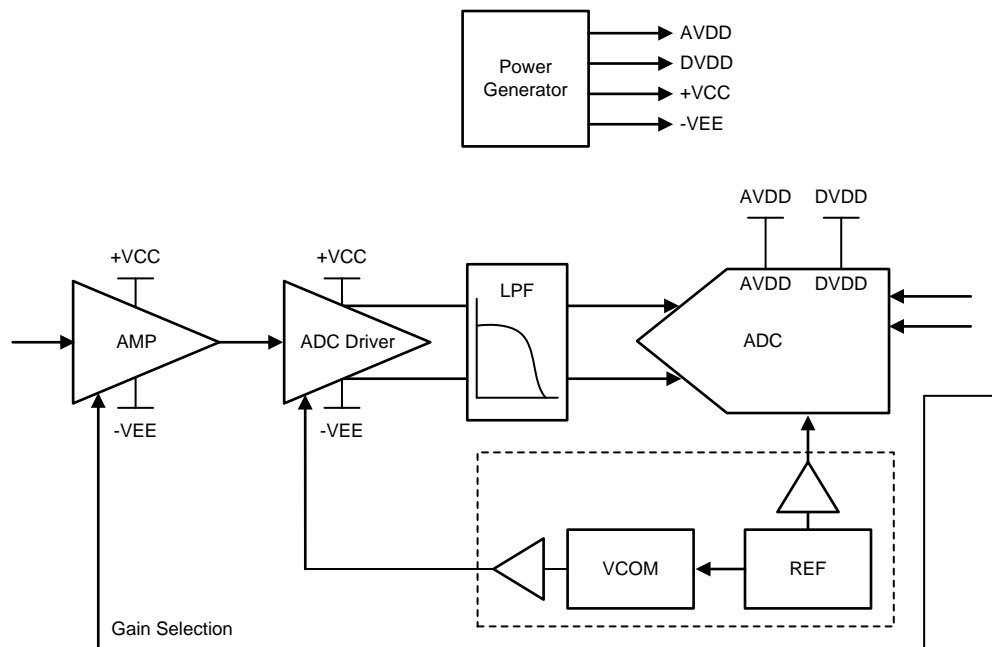


图 1. Generic AFE

### 1.1 Key System Specifications

表 1. Key System Specifications

PARAMETER	SPECIFICATIONS	MEASUREMENT
Number of channels	Dual	Dual
Input type	Differential	Differential
Input range	10- $V_{PP}$ fully differential	10- $V_{PP}$ fully differential
Resolution	20 bits	20 bits
SNR	> 100.13 dB	100.95 dB
THD	< -123 dB	-124.5 dB
ENOB	> 16.34 bit	16.47 bits

**表 1. Key System Specifications (continued)**

PARAMETER	SPECIFICATIONS	MEASUREMENT
System power	< 2.5 W	1.92 W
Form factor (L × W)	120 × 100 mm	112.98 × 99.82 mm

## 2 System Overview

### 2.1 Block Diagrams

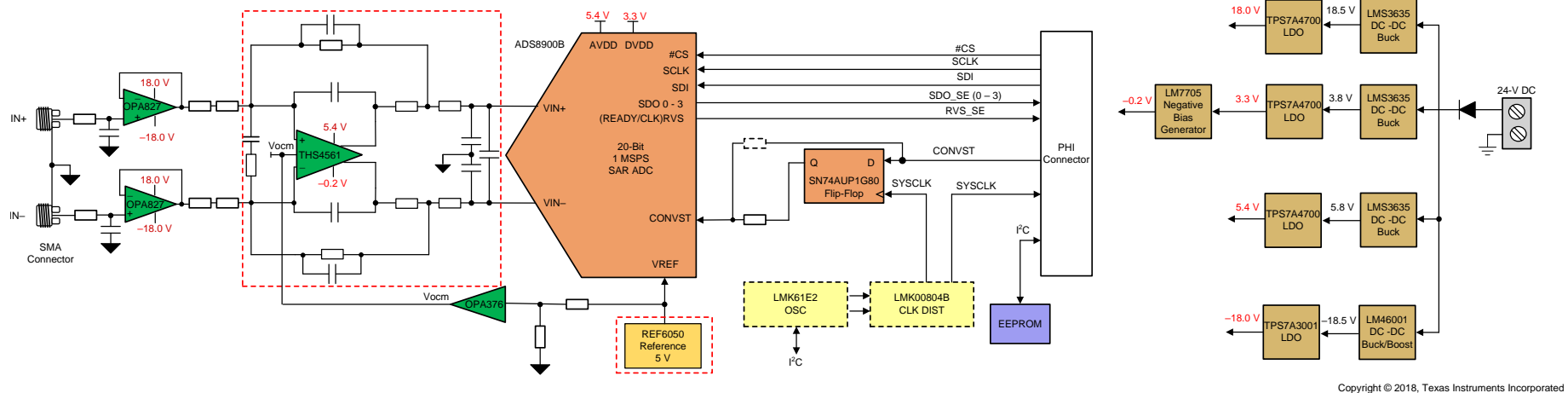


图 2. System Block Diagram

## 2.2 Highlighted Products

### 2.2.1 THS4561

The THS4561 FDA offers a simple interface from single-ended sources to the differential output required by high-precision ADCs. Designed for exceptional DC accuracy, low noise, and ultra-low harmonic distortion, the device is well suited for data acquisition systems where high precision is required with the best SNR and spurious-free dynamic range (SFDR) through the amplifier and ADC combination.

The THS4561 features the required negative rail input when interfacing a DC-coupled, ground-centered, source signal to a single-supply, differential-input ADC. Very-low DC error and drift terms support the emerging 16-bit to 20-bit SAR input requirements. A 2.85-V to 12.6-V supply range with a flexible output common-mode setting with low headroom to the supplies supports a wide range of ADC input and digital-to-analog converter (DAC) output requirements.

In this reference design, the THS4561 functions as a part of the ADC driver because it requires a high power supply range to realize the 10-V FSR.

### 2.2.2 REF6050

The REF6000 family of voltage references have an integrated, low-output impedance buffer that enable the user to directly drive the REF pin of precision data converters, while preserving linearity, distortion, and noise performance. Most precision SAR and delta-sigma ( $\Delta\Sigma$ ) ADCs switch binary-weighted capacitors onto the REF pin during the conversion process. To support this dynamic load, the output of the voltage reference must be buffered with a low-output impedance (high-bandwidth) buffer. The REF6000 family devices are well suited, but not limited, to drive the REF pin of the ADS88xx family of SAR ADCs, ADS127xx family of  $\Delta\Sigma$  ADCs, as well as other DACs.

The REF6000 family of voltage references are able to maintain an output voltage within 1 least significant bit (LSB), which is 18-bit, with minimal droop, even during the first conversion while driving the REF pin of the ADS8881 device. This feature is useful in burst-mode, event-triggered, equivalent-time sampling, and variable-sampling-rate data-acquisition systems. The REF60xx variants of the REF6000 family specify a maximum temperature drift of just 5 ppm/°C and initial accuracy of 0.05% for both the voltage reference and the low output impedance buffer, combined.

### 2.2.3 ADS8900B

The ADS8900B, ADS8902B, and ADS8904B (ADS890xB) belong to a family of pin-to-pin compatible, high-speed, single-channel, high-precision, 20-bit SAR ADCs with an integrated reference buffer and integrated LDO. The device family includes the ADS891xB (18-bit) and ADS892xB (16-bit) resolution variants.

The ADS89xxB boosts analog performance while maintaining high-resolution data transfer by using TI's Enhanced-SPI feature. Enhanced-SPI enables the ADS89xxB to achieve high throughput at lower clock speeds, which simplifies the board layout and lowers the overall system cost. Enhanced-SPI also simplifies the host's clocking-in of data, which makes it ideal for applications involving FPGAs and digital signal processors (DSPs). The ADS89xxB is compatible with a standard serial peripheral interface (SPI).

The ADS89xxB has an internal data parity feature which can be appended to the ADC data output. ADC data validation by the host, using parity bits, improves system reliability

## 2.3 System Design Theory

### 2.3.1 Power Structure

This system requires a wide variety of voltage rails to meet the specification of the reference design. The input voltage required for the system is 24-V DC. The power tree in [图 3](#) shows and highlights the distribution of the power into the different required rails. In this reference design, 5.4 V is generated to operate the REF6050 and THS4561 devices. The LM7705 device generates  $-0.2$  V so that the THS4561 device can swing rail to rail without distortion. For this reason, select an ADC driver amplifier such that its power supply voltage tolerance is over 5.6 V, which is the primary reason for using the THS4561 in this reference design. For a detailed design description of the entire power system, see [TIDA-01052](#) and [TIDA-01054](#).

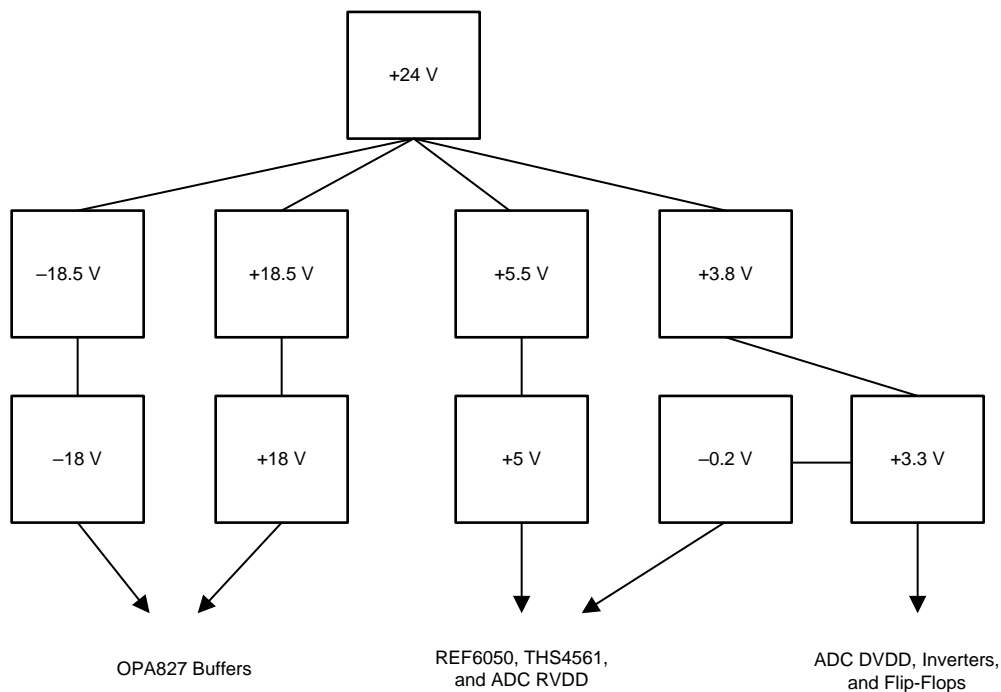


图 3. System Power Tree

### 2.3.2 ADC Driver Design Theory

The input driver circuit for a high-precision ADC mainly consists of two parts: a driving amplifier and a flywheel RC filter. The amplifier is used for signal conditioning of the input signal and its low output impedance provides a buffer between the signal source and the switched capacitor inputs of the ADC. The RC filter helps attenuate the sampling charge injection from the switched capacitor input stage of the ADC and functions as an antialiasing filter to band-limit the wideband noise contributed by the front-end circuit. Careful front-end circuit design is required to meet the resolution, linearity, and noise performance capabilities of the ADS8900B. The input operational amplifier (op amp) must support the following key specifications:

1. Rail-to-rail input and output (RRIO)
2. Low noise
3. High small-signal bandwidth with low distortion at high frequencies
4. Low power

For DC signals with fast transients that are common in a multiplexed application, the input signal must settle within a 20-bit accuracy at the device inputs during the acquisition time window. This condition is critical to maintain the overall linearity performance of the ADC. Typically, the amplifier data sheets specify the output settling performance only up to 0.1% to 0.001%, which may not be sufficient for the desired 20-bit accuracy. Therefore, the designer must verify the settling behavior of the input driver within a simulator, such as the TINA-TI™ simulation software, to help select the appropriate amplifier.

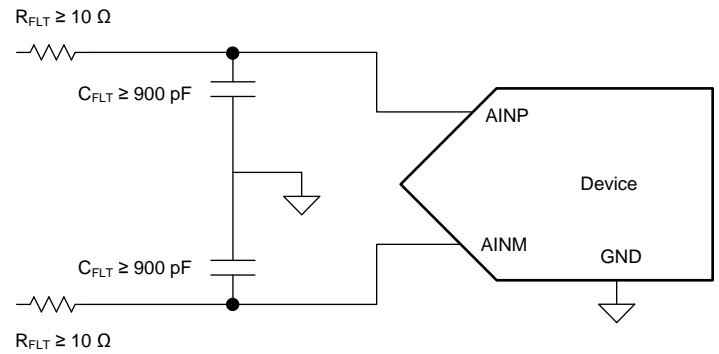
Converting analog-to-digital signals requires sampling an input signal at a constant rate. Any higher-frequency content in the input signal beyond half the sampling frequency is digitized and folded back into the low-frequency spectrum of interest, which is known as aliasing. Therefore, the designer must use an analog antialiasing filter to remove the noise and harmonic content from the input signal before the ADC performs sampling. An antialiasing filter is designed as a low-pass RC filter, where the 3-dB bandwidth is optimized based on specific application requirements.

For DC signals with fast transients (including multiplexed input signals), a high-bandwidth filter is designed to allow accurate settling of the signal at the inputs of the ADC during the small acquisition time window.

For AC signals, keeping the filter bandwidth low is desirable to band-limit the noise fed into the input of the ADC, thereby increasing the system SNR. Aside from filtering the noise from the front-end drive circuitry, the filter also helps attenuate the sampling charge injection from the switched-capacitor input stage of the ADC. A filter capacitor,  $C_{FLT}$ , is connected from each input pin of the ADC to the ground (as 公式 1 and 图 4 show).

This capacitor helps reduce the sampling charge injection and provides a charge bucket to quickly charge the internal sample-and-hold capacitors during the acquisition process. Generally, the value of this capacitor must be at least 15- to 20 times the specified sampling capacitor capacitance of the ADC. For example, TI's ADS8900B 20-bit SAR converter specification recommends to keep the  $C_{FLT}$  greater than 900 pF. However, the total harmonic distortion (THD) performance of the ADC driver amplifier typically degrades with high capacitive loads. Higher values of  $C_{FLT}$  also degrade the driver phase margin. Therefore, TI recommends to select the minimum required value of  $C_{FLT}$  and still maintain a good ratio between  $C_{FLT}$  and the ADC input sampling capacitance. This design uses a 1000-pF capacitor. The capacitor must be a COG- or NPO- type because these capacitor types have a high-Q, low-temperature coefficient, and stable electrical characteristics under varying voltages, frequency, and time.

$$f_{-3dB} = \frac{1}{2\pi \times R_{FLT} \times C_{FLT}} \quad (1)$$



Copyright © 2017, Texas Instruments Incorporated

图 4. Charge Kickback Filter

Note that driving capacitive loads can degrade the phase margin of their driving amplifiers, thus making the amplifier marginally unstable. To avoid amplifier stability issues, use series isolation resistors ( $R_{FLT}$  or  $R_{ISO}$ ) at the amplifier outputs. The resistor value is extremely important for many system parameters; see further discussion regarding these RC tradeoffs in [18-Bit , 1MSPS Data Acquisition Block \(DAQ\) Optimized for Lowest Distortion and Noise](#). A higher  $R_{FLT}$  value is helpful from the amplifier stability perspective, but adds distortion as a result of interactions with the nonlinear ADC input impedance. Distortion increases with source impedance, input signal frequency, and input signal amplitude. Therefore, the selection of  $R_{FLT}$  requires balancing the stability and distortion. For the ADS8900B, limiting the value of  $R_{FLT}$  to a maximum of  $10\ \Omega$  is recommended to avoid any significant degradation in linearity performance. The tolerance of the selected resistors must be kept less than 1% to keep the inputs balanced. The driver amplifier must be selected such that its closed-loop output impedance is at least five times less than the  $R_{FLT}$ .

### 2.3.2.1 THS4561 ADC Driver

Determine the values of  $R_{FLT}$  by comparing the THS4561 output impedance versus the ADC load impedance. 图 5 和 图 6 show the schematics used to simulate the ADC load impedance and the output impedance of THS4561, respectively. The simulation was done using TINA-TI.

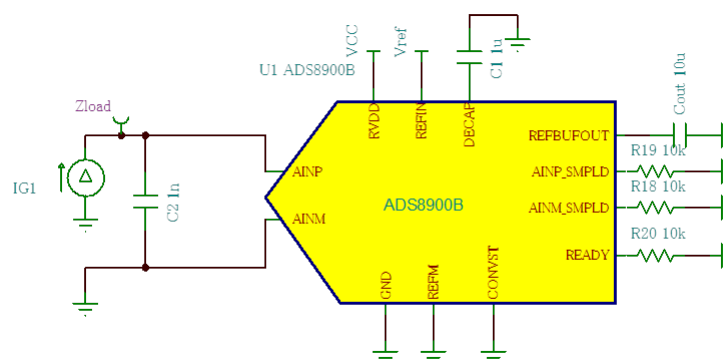


图 5. ADS8900B Load Impedance Simulation



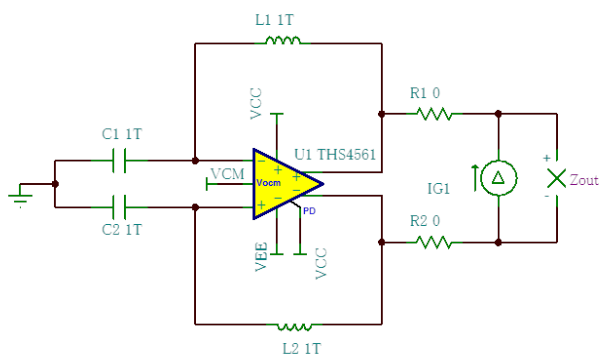


图 6. THS4561 Output Impedance Simulation

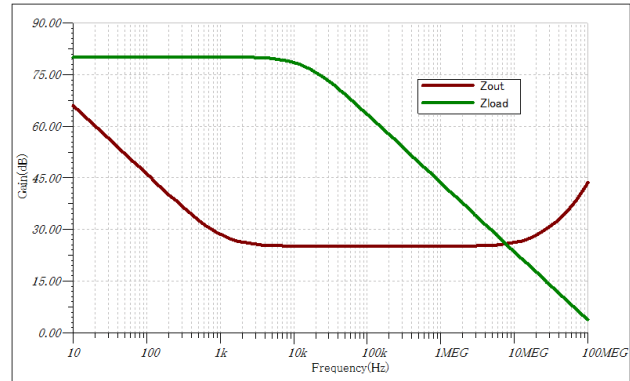


图 7.  $Z_{OUT}$  versus  $Z_{load}$  THS4561

As the simulation results in 图 7 show, the load impedance curve is falling while the output impedance curve is rising at the point of the intersection. This intersection at a rate of greater than 20 dB per decade can cause instability (oscillation) at the THS4561 output. To flatten the output impedance response to ensure stability, add a series output isolation resistance of 20  $\Omega$ .

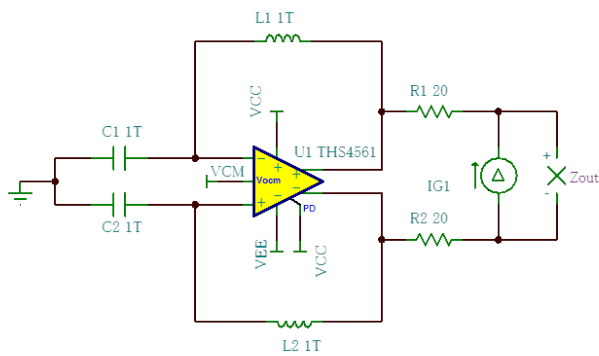


图 8. THS4561 with  $R_{iso}$

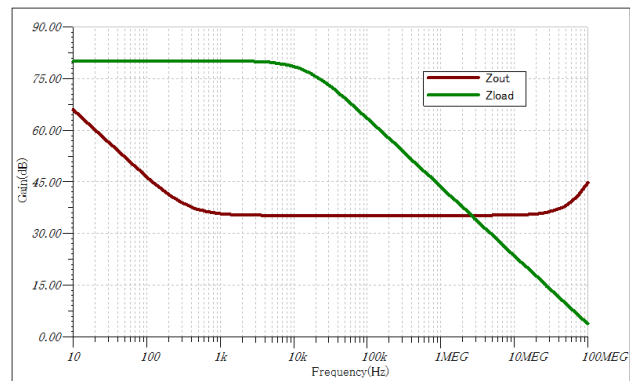


图 9. THS4561 With  $R_{iso}$  Compensation

图 9 shows the results of simulating the THS4561 output impedance after the isolation resistance was added. The load impedance curve crosses the output impedance curve at a frequency where the impedance is constant, which improves robustness.

图 10 is used to verify the stability of the THS4561 device. When evaluating the stability of the amplifier, be sure to confirm the closed-loop gain, loaded open-loop gain, and loop gain. The phase margin of the circuit is also crucial for circuit stability operation and required settling.

图 10 features 1TF capacitors and 1TH inductors for stability simulation. When measuring loaded open-loop gain and loop gain, the feedback loop must be broken. These components are used to properly break the feedback loop. Measuring the stability without these component is difficult because the offset causes saturation. DC-wise, the inductor is a short while the capacitor is an open. AC-wise, the inductor is an open and the capacitor is a short. This configuration breaks the feedback loop and allows the designer to measure the loaded open-loop gain and loop gain.

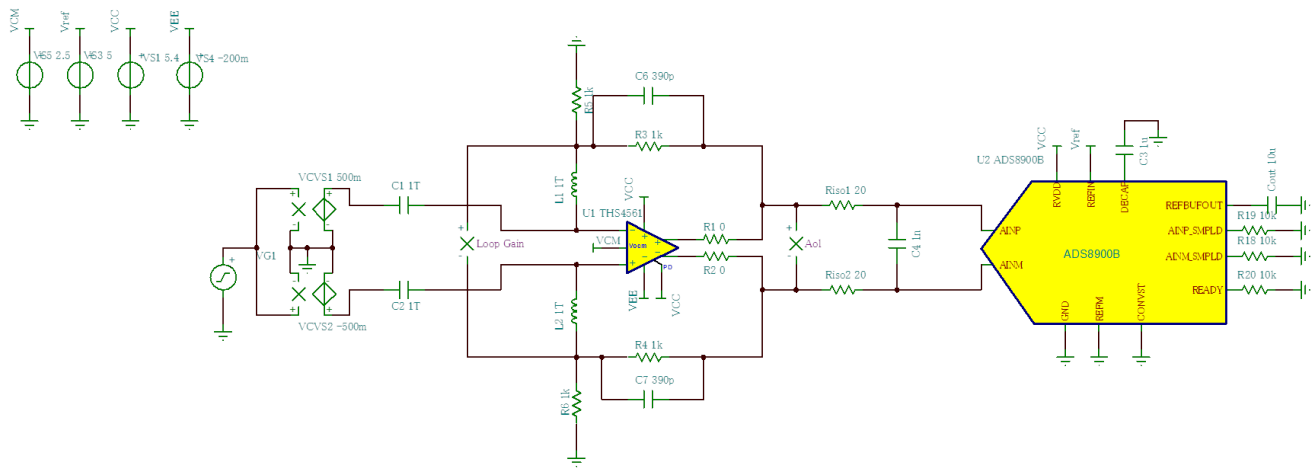


图 10. THS4561 Stability Schematic

图 11 显示 THS4561 稳定性模拟结果，指示在 38.9-MHz 单位增益频率处具有 43.79° 的相位裕量。

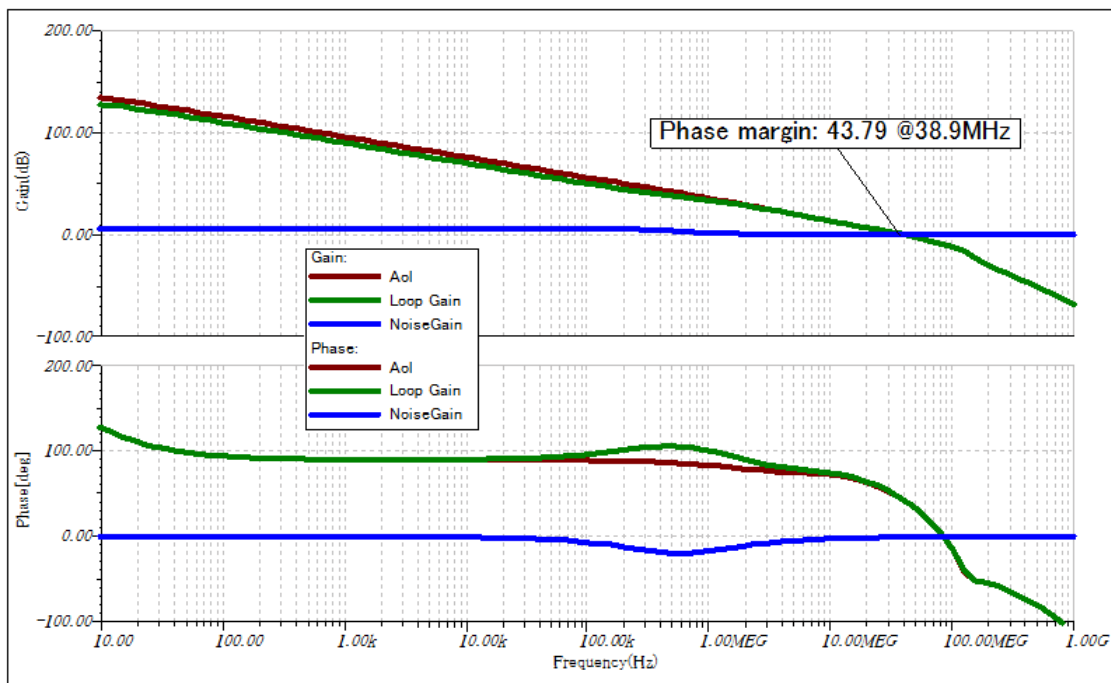
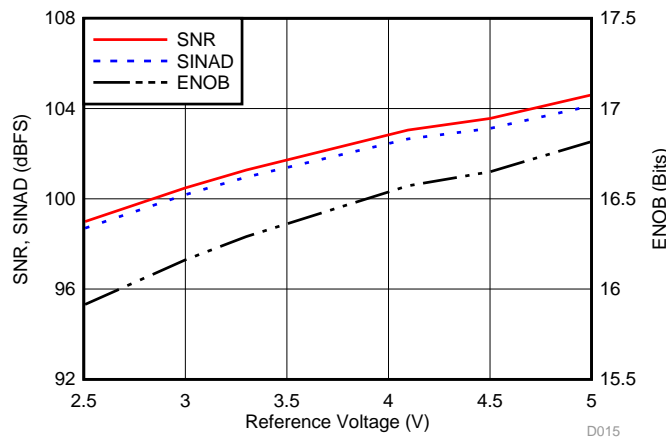


图 11. THS4561 Stability Results

### 2.3.2.2 Noise Analysis

This reference design focuses on an ADC driver, which ensures a 10-V<sub>PP</sub> differential input to the ADC. To achieve a 10-V<sub>PP</sub> differential input, use the THS4561 and REF6050. A comparison of the system (driver amplifier + ADC) noise performance with the traditional ADC driver (THS4551 and REF6041) is provided to validate the performance of this new ADC driver.

The [Analog Engineer's Calculator](#) allows the designer to calculate the system noise performance with ease. Calculating the system noise performance requires the designer to know the RMS noise of the amplifier, RMS noise of the reference voltage, and the SNR of the ADC. [REF60xx High-Precision Voltage Reference With Integrated ADC Drive Buffer](#) describes the RMS noise of the reference voltage and [ADS890xB 20-Bit, High-Speed SAR ADCs With Integrated Reference Buffer, and Enhanced Performance Features](#) describes the ADC SNR, and each values are 5 μV and 104.5 dBFS, respectively.



f<sub>IN</sub> = 2 kHz

图 12. ADS8900B Noise Performance versus Reference Voltage

图 13 和 图 14 显示 THS4551 和 THS4561 的噪声性能测量原理图。在图 13 中，R7 和 C5 用于稳定操作。ADS8900B 的仿真模型也放置在两个原理图中，以获得更准确的结果。TINA-TI 还用于获得两个放大器的总噪声。图 15 显示了测试结果。

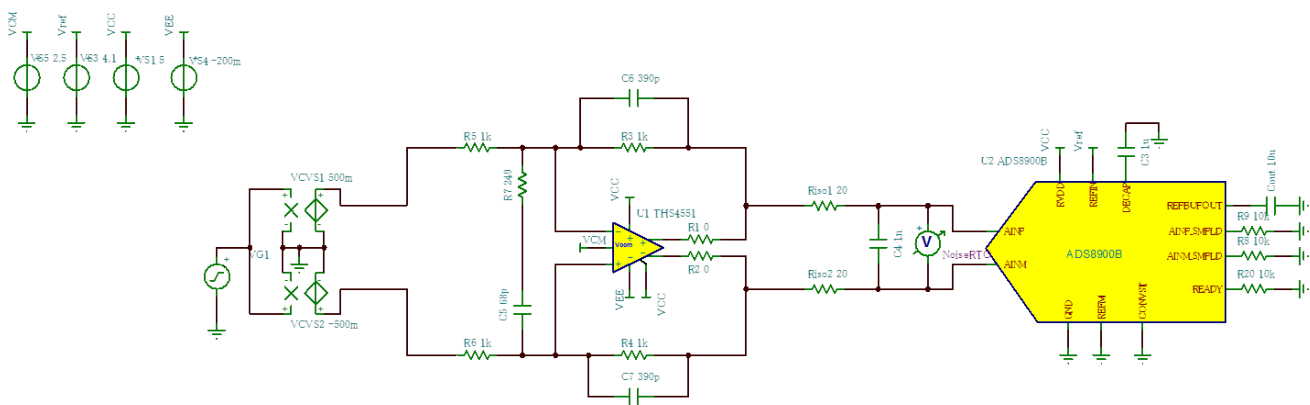


图 13. THS4551 Schematic for Noise Simulation

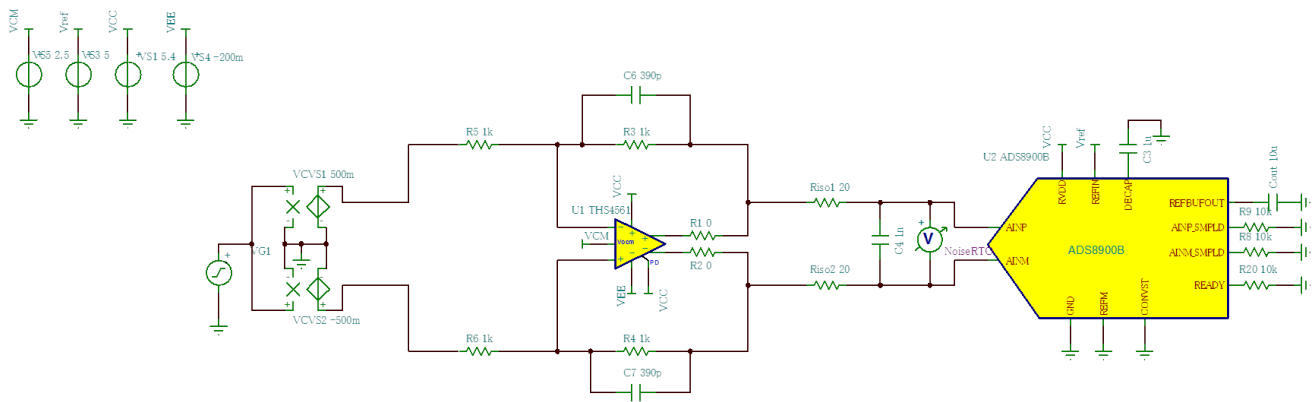


图 14. THS4561 Schematic for Noise Simulation

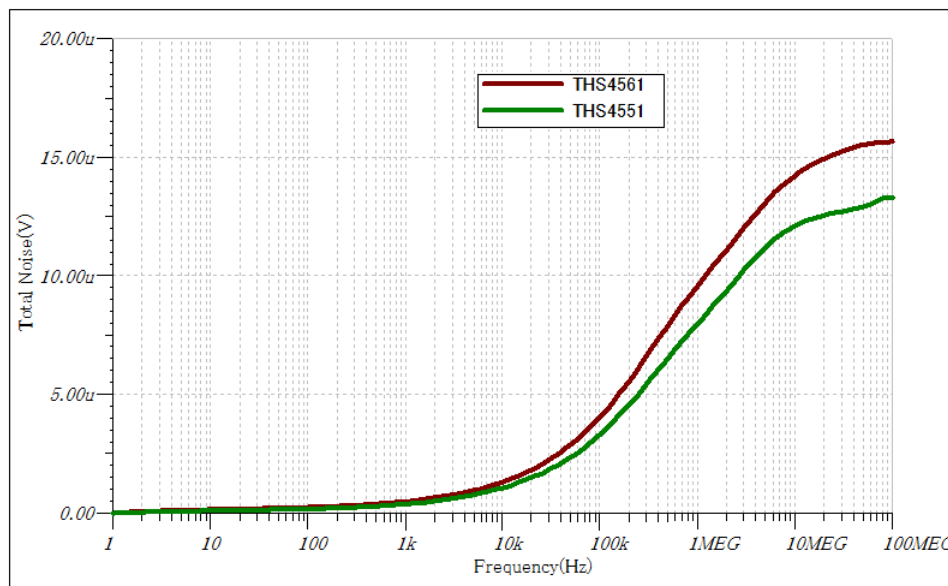


图 15. Total Noise Comparison

From 图 15, the total noise of THS4551 and THS4561 was 13.29  $\mu\text{V}$  and 15.63  $\mu\text{V}$ , respectively. Therefore, the THS4561 is inferior to the THS4551 when considering just the noise of the amplifier. A trade-off between the quiescent current and noise is the cause of this parameter. The THS4561 has a lower quiescent current (0.82 mA) than the THS4551 (1.35 mA).

Now, calculate the system noise performance by using the [Analog Engineer's Calculator](#). 图 16 and 图 17 show the results for THS4551 + REF6041 and THS4561 + REF6050, respectively. Note that, because the ADS8900B has a true differential input, the FSR changes to double that of the reference voltage. Thus, the FSR from REF6041 (4.096-V output) is 8.192 V. Similarly, the FSR from REF6050 (5-V output) is 10 V. For further detail, see the section regarding ADC Transfer Function in [ADS890xB 20-Bit, High-Speed SAR ADCs With Integrated Reference Buffer, and Enhanced Performance Features](#). From 图 12, the ADC SNR with reference voltages of 4.096 V and 5 V can be recognized as 103.5 dB and 104.5 dB roughly. As a result, the system noise performance of the THS4561 outperforms the THS4551 by 0.8 dB, even though the noise performance of the THS4561 itself is inferior to the THS4551.

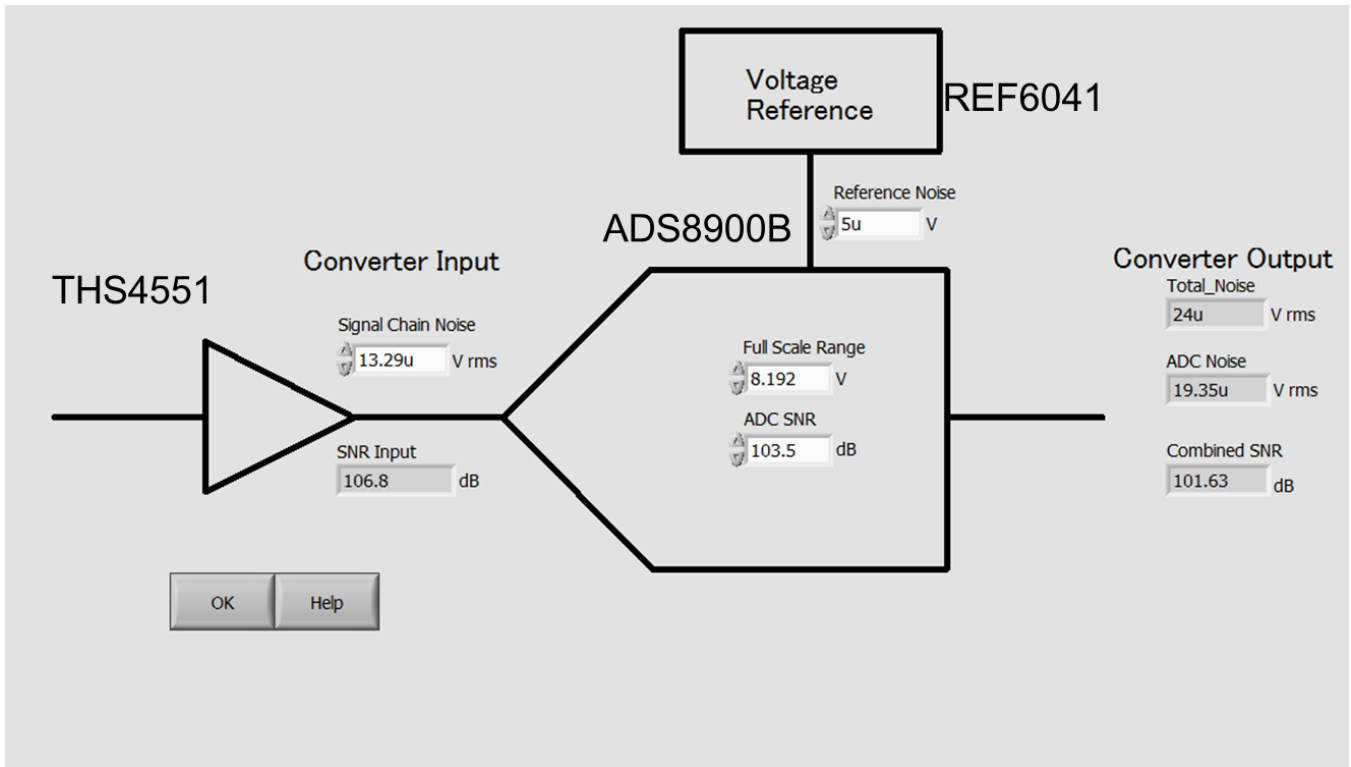


图 16. System Noise Calculation for THS4551 + REF6041

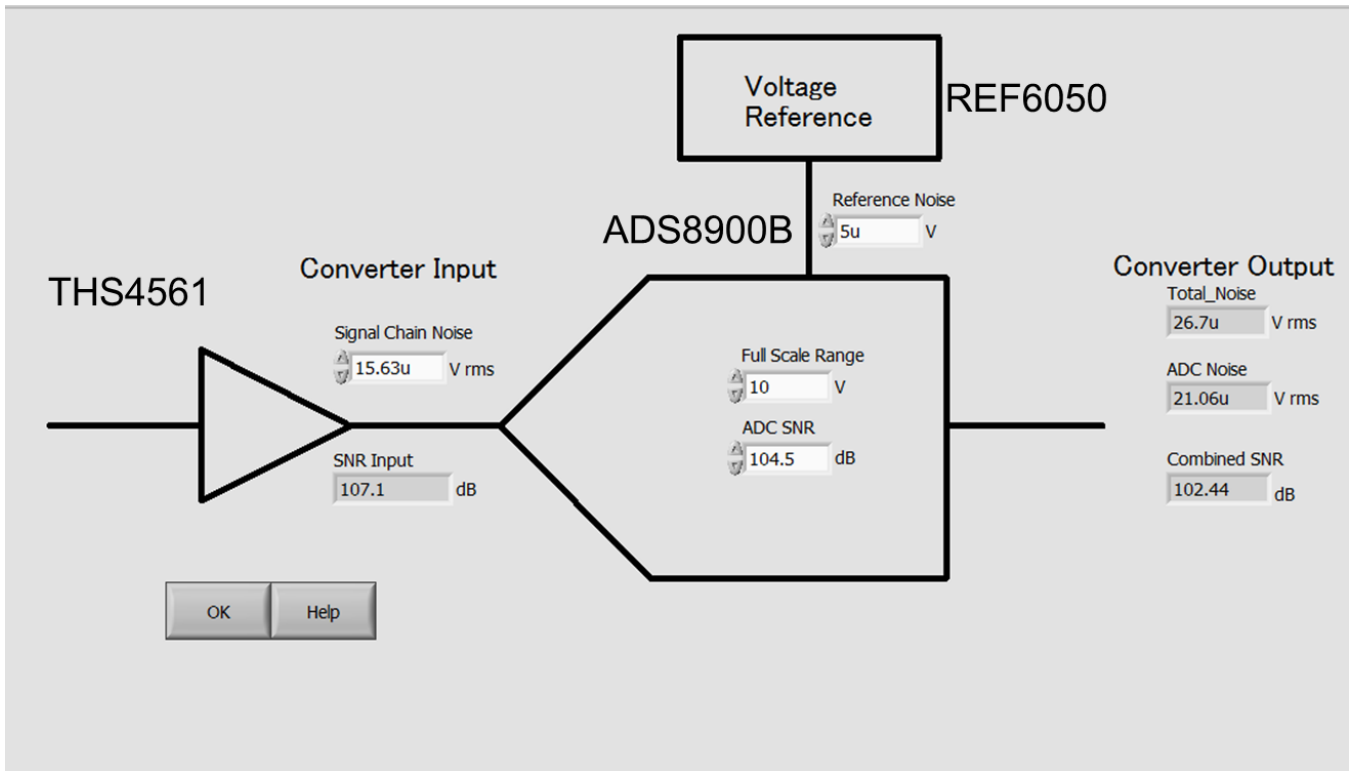


图 17. System Noise Calculation for THS4561 + REF6050

### 3 Hardware, Software, Testing Requirements, and Test Results

#### 3.1 Required Hardware

The following subsection outlines the information for getting the board up and running as fast as possible. To learn about the PHI board or the onboard clocking and jitter cleaner, see [Optimized Analog Front-End DAQ System Reference Design for 18-Bit SAR Data Converters](#). Take care when moving the jumper pins to avoid possible damage to the components.

##### 3.1.1 Jumper Configuration

This system has several configurable power options. These options are selectable by using two-pin and three-pin jumpers. 表 2 highlights the purpose of each jumper and assists in changing the configuration to fit the needs of the user.

表 2. Jumper Configuration

JUMPER NAME	SHORT PINS 1 AND 2	SHORT PINS 2 AND 3	DEFAULT CONFIGURATION
JSI_18V	Power to LMS3635-Q1 18-V rail	—	Short
JTI_18V	Connects LMS3635-Q1 to TPS7A700 for 18-V rail	Connects LMZ14201 to TPS7A700 for 18-V rail	Short pins 1 and 2
JSI_5V	Power to LMS3635-Q1 5-V rail	—	Short
JTI_5V	Connects LMS3635-Q1 to TPS7A700 for 5-V rail	Connects LMZ14203 to TPS7A700 for 5-V rail	Short pins 1 and 2
JSI_3.3V	Power to LMS3635-Q1 3.3-V rail	—	Short
JTI_3.3V	Connects LMS3635-Q1 to TPS7A700 for 3.3-V rail	Connects LMZ14202 to TPS7A700 for 3.3-V rail	Short pins 1 and 2
JPRI_–18V	Power to LM46001 –18-V rail	—	Short
JTI_–18V	Connects LM46001 to TPS7A3001 for –18-V rail	Connects LM5574 to TPS7A3001 for –18-V rail	Short pins 1 and 2
JMTI_–18V	Power to LM5574 –18-V rail	—	Open
JZI_18V	Power to LMZ14201 18-V rail	—	Open
JZI_3.3V	Power to LMZ14202 3.3-V rail	—	Open
JZI_5V	Power to LMZ14203 5-V rail	—	Open
J39	Connects –0.2-V rail to OPA625 and THS4561	Shorts –0.2-V rail to ground	Short pins 1 and 2

### 3.2 Testing and Results

An Audio Precision 2700 series signal generator is used as the signal source to test the AFE and ADC performance. The noise and THD of the AP2700 have adequate performance and do not limit measurements or system performance. Use of a quality source is crucial to avoid limiting the system's performance by the signal source. A generic DC power supply was used to generate the 18.5-V DC, -18.5-V DC, 5.8-V DC, 3.8-V DC, and -0.25-V DC. The AP2700 is set to output a 2-kHz sinusoid. A value of 2 kHz is chosen because it is the standard frequency in measuring noise and THD. The amplitude for THS4551 was chosen as  $8 V_{PK-PK}$  to grant the full range on it. A  $9.16-V_{PK-PK}$  amplitude was chosen for THS4561 due to the constraint of the signal generator.

A PHI controller board is used to connect the TIDA-01057 board to the host PC, where the ADS8900B EVM GUI is running. This software measures the SNR, THD, SFDR, signal-to-noise distortion ratio (SINAD), and effective number of bits (ENOB) for the ADC by running a spectral analysis.

图 18 和 图 19 显示 THS4551 + REF6041 和 THS4561 + REF6050 的测试结果。表 3 总结了每个规格。如前图 16 和 图 17 所示，SNR 提高了约 0.8 dB。此外，THS4561 在所有其他规格上都超过了 THS4551，如表 3 所示。请注意，某些噪声分量，例如相位噪声、开关噪声和第一阶段缓冲器噪声，在之前的计算中并未考虑，这就是为什么实际测量值略低于计算值的原因。总之，THS4561 允许设计者改善整个系统的噪声性能和功耗，即使其噪声性能不如 THS4551。

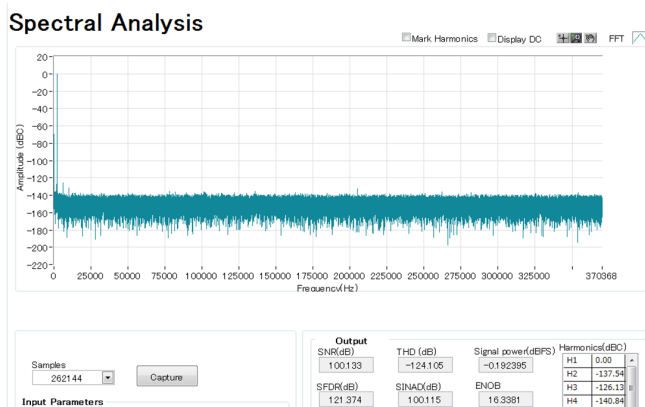


图 18. THS4551 Results

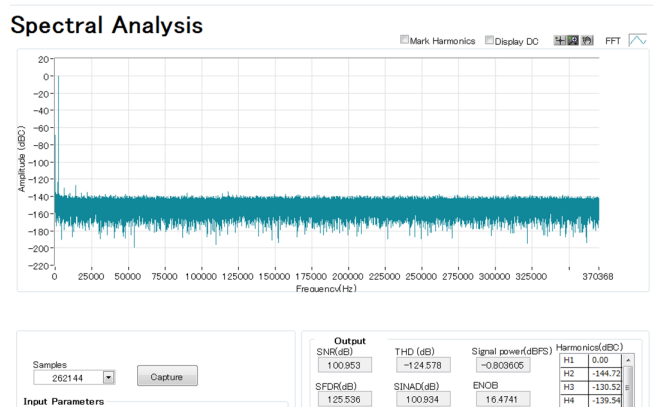


图 19. THS461 Results

表 3. Comparison of Test Results

SPECIFICATION	THS4551	THS4561
SNR	100.13 dB	100.95 dB
THD	-124.11 dB	-124.57 dB
ENOB	16.3	16.4
SFDR	121.3 dB	125.5 dB

## 4 Design Files

### 4.1 Schematics

To download the schematics, see the design files at [TIDA-01057](#).

### 4.2 Bill of Materials

To download the bill of materials (BOM), see the design files at [TIDA-01057](#).

### 4.3 PCB Layout Recommendations

#### 4.3.1 Layout Prints

To download the layer plots, see the design files at [TIDA-01057](#).

### 4.4 Altium Project

To download the Altium project files, see the design files at [TIDA-01057](#).

### 4.5 Gerber Files

To download the Gerber files, see the design files at [TIDA-01057](#).

### 4.6 Assembly Drawings

To download the assembly drawings, see the design files at [TIDA-01057](#).

## 5 Software Files

To download the software files, see the design files at [TIDA-01057](#).

## 6 Related Documentation

1. Texas Instruments, [Multi-Rail Power Reference Design for Eliminating EMI Effects in High-Performance DAQ Systems](#)
2. Texas Instruments, [REF60xx High-Precision Voltage Reference With Integrated ADC Drive Buffer](#)
3. Texas Instruments, [ADS890xB 20-Bit, High-Speed SAR ADCs With Integrated Reference Buffer, and Enhanced Performance Features](#)
4. Texas Instruments, [Optimized Analog Front-End DAQ System Reference Design for 18-Bit SAR Data Converters](#)

### 6.1 商标

E2E, TINA-TI are trademarks of Texas Instruments.

## 7 About the Authors

**SHOTA MAGO** is a field application engineer at Texas Instruments, where he is responsible for supporting Japanese industrial companies and proposing solutions for them. Shota obtained his bachelor's degree and master of electrical and electronic engineering from the University of Miyazaki in Japan.



**TARAS DUDAR** is a systems design engineer and architect at Texas Instruments, where he is responsible for developing reference design solutions for the test and measurement industry. Previously, Taras designed high-speed analog SOC integrated circuits for Gbps data communications. Taras has earned his master of science in electrical engineering (MSEE) degree from the Oregon State University in Corvallis, OR.

## 有关 TI 设计信息和资源的重要通知

德州仪器 (TI) 公司提供的技术、应用或其他设计建议、服务或信息，包括但不限于与评估模块有关的参考设计和材料（总称“TI 资源”），旨在帮助设计人员开发整合了 TI 产品的应用；如果您（个人，或如果是代表贵公司，则为贵公司）以任何方式下载、访问或使用了任何特定的 TI 资源，即表示贵方同意仅为该等目标，按照本通知的条款进行使用。

TI 所提供的 TI 资源，并未扩大或以其他方式修改 TI 对 TI 产品的公开适用的质保及质保免责声明；也未导致 TI 承担任何额外的义务或责任。TI 有权对其 TI 资源进行纠正、增强、改进和其他修改。

您理解并同意，在设计应用时应自行实施独立的分析、评价和判断，且应全权负责并确保应用的安全性，以及您的应用（包括应用中使用的 TI 产品）应符合所有适用的法律法规及其他相关要求。就您的应用声明，您具备制订和实施下列保障措施所需的一切必要专业知识，能够 (1) 预见故障的危险后果，(2) 监视故障及其后果，以及 (3) 降低可能导致危险的故障几率并采取适当措施。您同意，在使用或分发包含 TI 产品的任何应用前，您将彻底测试该等应用和该等应用所用 TI 产品的功能而设计。除特定 TI 资源的公开文档中明确列出的测试外，TI 未进行任何其他测试。

您只有在为开发包含该等 TI 资源所列 TI 产品的应用时，才被授权使用、复制和修改任何相关单项 TI 资源。但并未依据禁止反言原则或其他法律授予您任何 TI 知识产权的任何其他明示或默示的许可，也未授予您 TI 或第三方的任何技术或知识产权的许可，该等许可包括但不限于任何专利权、版权、屏蔽作品权或与使用 TI 产品或服务的任何整合、机器制作、流程相关的其他知识产权。涉及或参考了第三方产品或服务的信息不构成使用此类产品或服务的许可或与其相关的保证或认可。使用 TI 资源可能需要您向第三方获得对该等第三方专利或其他知识产权的许可。

TI 资源系“按原样”提供。TI 兹免除对 TI 资源及其使用作出所有其他明确或默示的保证或陈述，包括但不限于对准确性或完整性、产权保证、无屡发故障保证，以及适销性、适合特定用途和不侵犯任何第三方知识产权的任何默认保证。

TI 不负责任何申索，包括但不限于因组合产品所致或与之有关的申索，也不为您辩护或赔偿，即使该等产品组合已列于 TI 资源或其他地方。对因 TI 资源或其使用引起或与之有关的任何实际的、直接的、特殊的、附带的、间接的、惩罚性的、偶发的、从属或惩戒性损害赔偿，不管 TI 是否获悉可能会产生上述损害赔偿，TI 概不负责。

您同意向 TI 及其代表全额赔偿因您不遵守本通知条款和条件而引起的任何损害、费用、损失和/或责任。

本通知适用于 TI 资源。另有其他条款适用于某些类型的材料、TI 产品和服务的使用和采购。这些条款包括但不限于适用于 TI 的半导体产品 (<http://www.ti.com/sc/docs/stdterms.htm>)、[评估模块](http://www.ti.com/sc/docs/sampters.htm)和样品 (<http://www.ti.com/sc/docs/sampters.htm>) 的标准条款。

邮寄地址：上海市浦东新区世纪大道 1568 号中建大厦 32 楼，邮政编码：200122  
Copyright © 2018 德州仪器半导体技术（上海）有限公司